19. Wu S, Kanda T, Imazeki F, et al. Hepatitis B virus e antigen downregulates cytokine production in human hepatoma cell lines. Viral Immunol. 2010; 23: 467-476.
20. Usuda S, Okamoto H, Iwanari H, et al. Serological detection of hepatitis B virus genotypes by ELISA with monoclonal antibodies to type-specific epitopes in the preS2-region product. J Virol Methods. 1999; 80: 97-112.
21. Gallego A, Sheldon J, Garcia-Samaniego J, et al. Evaluation of initial virological response to adefovir and development of adefovir-resistant mutations in patients with chronic hepatitis B. J Viral Hepat. 2008; 15: 392-398.
22. Fujiwara K, Yokosuka O, Ehata T, et al. The two different states of hepatitis B virus DNA in asymptomatic carriers: HBe-antigen-positive versus anti-HBe-positive asymptomatic carriers. Dig Dis Sci. 1998; 43: 368-376.
23. Mendes-Correa MC, Pinho JR, Gomes-Gouvea MS, et al. Predictors of HBeAg status and hepatitis B viremia in HIV-infected patients with chronic hepatitis B in the HAART era in Brazil. BMC Infect Dis. 2011; 11: 247.
24. Wong VW, Wong GL, Yiu KK, et al. Entecavir treatment in patients with severe acute exacerbation of chronic hepatitis B. J Hepatol. 2011; 54: 236-242.
25. Sarin SK, Sandhu BS, Sharma BC, et al. Beneficial effects of 'lamivudine pulse' therapy in HBeAg-positive patients with normal ALT. J Viral Hepat. 2004; 11: 552-558.
26. Fujisaki S, Yokomaku Y, Shiino T, et al. Outbreak of infections by hepatitis B virus genotype A and transmission of genetic drug resistance in patients coinfected with HIV-1 in Japan. J Clin Microbiol. 2011; 49: 1017-1024.
27. Lindh M, Uhnoo I, Blackberg J, et al. Treatment of chronic hepatitis B infection: An update of Swedish recommendations. Scand J Infect Dis. 2008; 40: 436-450.
28. Seta T, Yokosuka O, Imazeki F, et al. Emergence of YMDD motif mutants of hepatitis B virus during lamivudine treatment of immunocompetent type B hepatitis patients. J Med Virol. 2000; 60: 8-16.
29. Kusumoto S, Tanaka Y, Ueda R, et al. Reactivation of hepatitis B virus following rituximab-plus-steroid combination chemotherapy. J Gastroenterol. 2011; 46: 9-16.
30. Yeo W, Johnson PJ. Diagnosis, prevention and management of hepatitis B virus reactivation during anticancer therapy. Hepatology. 2006; 43: 209-220.

Hepatitis B Virus e Antigen Physically Associates With Receptor-Interacting Serine/Threonine Protein Kinase 2 and Regulates *IL-6* Gene Expression

Shuang Wu,[1] Tatsuo Kanda,[1] Fumio Imazeki,[1] Shingo Nakamoto,[1,2] Takeshi Tanaka,[1,3] Makoto Arai,[1] Thierry Roger,[5] Hiroshi Shirasawa,[2] Fumio Nomura,[4] and Osamu Yokosuka[1]

[1]Department of Medicine and Clinical Oncology, [2]Department of Molecular Virology, [3]Department of Environment Biochemistry, and [4]Department of Molecular Diagnosis, Graduate School of Medicine, Chiba University, Japan; and [5]Infectious Diseases Service, Department of Medicine, Centre Hospitalier Universitaire Vaudois and University of Lausanne, Lausanne, Switzerland

We previously reported that hepatitis B virus (HBV) e antigen (HBeAg) inhibits production of interleukin 6 by suppressing NF-κB activation. NF-κB is known to be activated through receptor-interacting serine/threonine protein kinase 2 (RIPK2), and we examined the mechanisms of interleukin 6 regulation by HBeAg. HBeAg inhibits RIPK2 expression and interacts with RIPK2, which may represent 2 mechanisms through which HBeAg blocks nucleotide-binding oligomerization domain-containing protein 1 ligand–induced NF-κB activation in HepG2 cells. Our findings identified novel molecular mechanisms whereby HBeAg modulates intracellular signaling pathways by targeting RIPK2, supporting the concept that HBeAg could impair both innate and adaptive immune responses to promote chronic HBV infection.

Hepatitis B virus (HBV) nucleoprotein exists in 2 forms [1, 2]. Nucleocapsid, designated HBV core antigen (HBcAg), is an intracellular, 21-kDa protein that self-assembles into particles that encapsidate viral genome and polymerase and is essential for function and maturation of virion. HBV also secretes a nonparticle second form of the nucleoprotein, designated precore or HBV e antigen (HBeAg) [1, 2]. Precore and core proteins are translated from 2 RNA species that have different 5′ initiation sites. Precore messenger RNA (mRNA) encodes a hydrophobic signal sequence that directs precore protein to the endoplasmic reticulum, where it undergoes N- and C-terminal cleavage within the secretory pathway and is secreted as an 18-kDa monomeric protein [3–5].

Nucleotide-binding oligomerization domain–containing protein 1 (NOD1) and NOD2 are cytosolic pattern-recognition receptors involved in the sensing of bacterial peptidoglycan subcomponents [6]. NOD1 and NOD2 stimulation activates NF-κB through receptor-interacting serine/threonine protein kinase 2 (RIPK2; also known as RIP2, RICK, or CARDIAK), a caspase-recruitment domain-containing kinase. RIPK2 is also involved in Toll-like receptor (TLR)–signaling pathway and plays an important role in the production of inflammatory cytokines through NF-κB activation [6, 7].

We previously reported that HBeAg inhibits the production of interleukin 6 (IL-6) through suppression of NF-κB activation [4]. In the present study, we investigated the molecular mechanism of HBeAg functions for the requirement of RIPK2 in NF-κB transcriptional regulation.

METHODS

Cell Culture and Plasmids

HepG2, Huh7, HT1080, COS7, and HEK293T cells were used in the present study. Stable cell lines were obtained as previously described [4]. Briefly, HepG2, Huh7, and HT1080 were transfected with pCXN2-HBeAg(+) or pCXN2-HBeAg(−) in Effectene (Qiagen). After G418 screening, HBeAg-positive and -negative HepG2/Huh7/HT1080 cell lines were collected for further analysis [4]. The plasmid pCXN2-HBeAg(+), which can produce both HBeAg and core peptides, and the plasmid pCXN2-HBeAg(−), which can produce only core peptides, were obtained as described previously [4]. pNF-κB–luc, which expresses luciferase upon promoter activation by NF-κB, was purchased from Stratagene [4]. pGFP–human RIPK2 (kindly provided by Prof John C. Reed, Sanford-Burnham Institute for Medical Research) can express GFP-human $RIP2^{WT}$ [8].

HepG2 cells were transfected with plasmid control–small hairpin RNA (shRNA) or with RIPK2-shRNA (Santa Cruz). After puromycin screening, individual colonies were picked up and examined for expression of endogenous RIPK2, and clones HepG2-shC and HepG2-shRIPK2-3 were selected for subsequent studies.

Received 1 January 2012; accepted 3 February 2012; electronically published 21 May 2012.
Correspondence: Tatsuo Kanda, MD, PhD, Department of Medicine and Clinical Oncology, Chiba University, Graduate School of Medicine, 1-8-1 Inohana, Chuo-ku, Chiba 260-8670, Japan (kandat-cib@umin.ac.jp).

The Journal of Infectious Diseases 2012;206:415–20

DOI: 10.1093/infdis/jis363

Luciferase Assays and Treatment of Cells With NOD Ligands

Around 1.0×10^5 HepG2 and Huh7 cells were plated in 6-well plates (Iwaki Glass, Tokyo, Japan) for 24 hours and transfected with 0.4 μg of pNF-κB–luc. For luciferase assay of NF-κB activation, cells were treated for 4 hours with or without NOD1 ligand (C12-iEDAP, 2.5 μg/mL) and NOD2 ligand (muramyl dipeptide [MDP], 10 μg/mL) (InvivoGen) at 44 hours after transfection [9]. After 48 hours, cells were lysed with reporter lysis buffer (Promega), and luciferase activity was determined as described previously [4].

RNA Extraction, Complementary DNA (cDNA) Synthesis, Real-Time Polymerase Chain Reaction (PCR) Analysis, and PCR Array

Total RNA was isolated by RNeasy Mini Kit (Qiagen). A total of 5 μg of RNA was reverse transcribed using the First Strand cDNA Synthesis Kit (Qiagen) [4]. Quantitative amplification of cDNA was monitored with SYBR Green by real-time PCR in a 7300 Real-Time PCR system (Applied Biosystems). Gene expression profiling of 84 TLR-related genes was performed using RT^2 profiler PCR arrays (Qiagen) in accordance with the manufacturer's instructions [4].

Gene expression was normalized to 2 internal controls (GAPDH and/or β-actin) to determine the fold-change in gene expression between the test sample (HBeAg-positive HepG2/Huh7/HT1080) and the control sample (HBeAg-negative HepG2/Huh7/HT1080) by the 2^{-ddCT} (comparative cycle threshold) method [4]. Three sets of real-time PCR arrays were performed. Some results of HepG2 cells were previously reported [4].

Coimmunoprecipitation

Cells were cotransfected with 2.5 μg pCXN2-HBeAg(+) or 2.5 μg pCXN2-HBeAg(−), as well as with 2.5 μg pGFP–human RIPK2, and cell lysates were prepared after 48 hours, using lysis buffer containing a cocktail of protease inhibitors. Cell lysates were incubated with anti-GFP rabbit polyclonal antibody (Santa Cruz) or anti-HBe mouse monoclonal antibody (Institute of Immunology, Tokyo, Japan) for 3 hours at 4°C, followed by overnight incubation with protein G–Sepharose beads (Santa Cruz). Immunoprecipitates were separated by sodium dodecyl sulfate–polyacrylamide gel electrophoresis and electroblotted onto a nitrocellulose membrane. Immunoblotting was performed by incubating the membrane for 1 hour with anti-HBe antibody. Proteins were detected by enhanced chemiluminescence (GE Healthcare), using an image analyzer (LAS-4000, Fuji Film). The membrane was reprobed with a monoclonal antibody to GFP or RIPK2 (Cell Signaling).

Transfection of pGFP–Human RIPK2 and Confocal Microscopy

Formaldehyde (3.7%)–fixed cells were incubated with anti-HBe antibody and stained with fluorochrome-conjugated secondary antibody (Alexa Fluor 555 conjugate, Cell Signaling). Cells were mounted for confocal microscopy (ECLIPSE TE 2000-U, Nikon). Whenever necessary, images were merged digitally to monitor colocalization. Cotransfection of 0.1 μg pCXN2-HBeAg(+) or 0.1 μg pCXN2-HBeAg(−) with 0.3 μg pGFP–human RIPK2 into the cells was performed. After 48 hours, intracellular localization of RIPK2 was visualized by confocal microscopy.

Enzyme-Linked Immunosorbent Assay (ELISA) for IL-6

Cell culture fluid was analyzed for IL-6 by ELISA (KOMA-BIOTECH, Seoul, Korea), in accordance with the manufacturer's protocol [4].

Small Interfering RNA (siRNA) Transfection and Wound-Healing Assay

Control siRNA (siC) and siRNA specific for RIPK2 (siRIPK2) were purchased from Thermo Fisher Scientific. Cells were transfected with siRNA by electroporation. After 48 hours, cells were treated with 10 ng/mL tumor necrosis factor α (TNF-α) (Wako Pure Chemical, Osaka, Japan), while the wound-healing (ie, scratch) assay was performed using a p-200 pipette tip to induce RIPK2 [10]. Up to 12 hours after scratching, the cells were observed by microscopy. Cell migration was measured using Scion Images (SAS). Migration by siC-transfected cells was set at 1.

Statistical Analysis

Results are expressed as mean values ± SD. The Student *t* test was used to determine statistical significance.

RESULTS

HBeAg Downregulates RIPK2 Expression

To explore the effect of HBeAg on TLR-related gene expression, we generated HepG2, Huh7, and HT1080 cell lines that stably expressed HBV core region with or without precore region. HT1080, a primate fibrosarcoma cell line, is useful for the study of interferon signaling. HBeAg and HBV core–related antigen (HBcrAg) levels of these cell lines demonstrated that expression of HBV core region without HBV precore region did not allow HBeAg secretion by cells (data are cited elsewhere [4] or not shown). First, we performed real-time RT-PCR analysis of these cell lines, using focused gene arrays (Figure 1*A*). We observed that, in 3 cell lines, 5 genes (*RIPK2, TLR9, TNF, CD180,* and *IL1A*) were downregulated ≥1.3-fold in HBeAg-positive cells than in HBeAg-negative cells. We chose to focus our investigation on RIPK2 because HBeAg inhibits the production of IL-6 through the suppression of NF-κB activation [4], and NF-κB is known to be activated through RIPK2 [4]. RIPK2 expression was >100-, 1.41-, and 1.45-fold lower in HBeAg-positive HepG2, Huh7, and HT1080 cells, respectively, compared with their HBeAg-negative counterparts

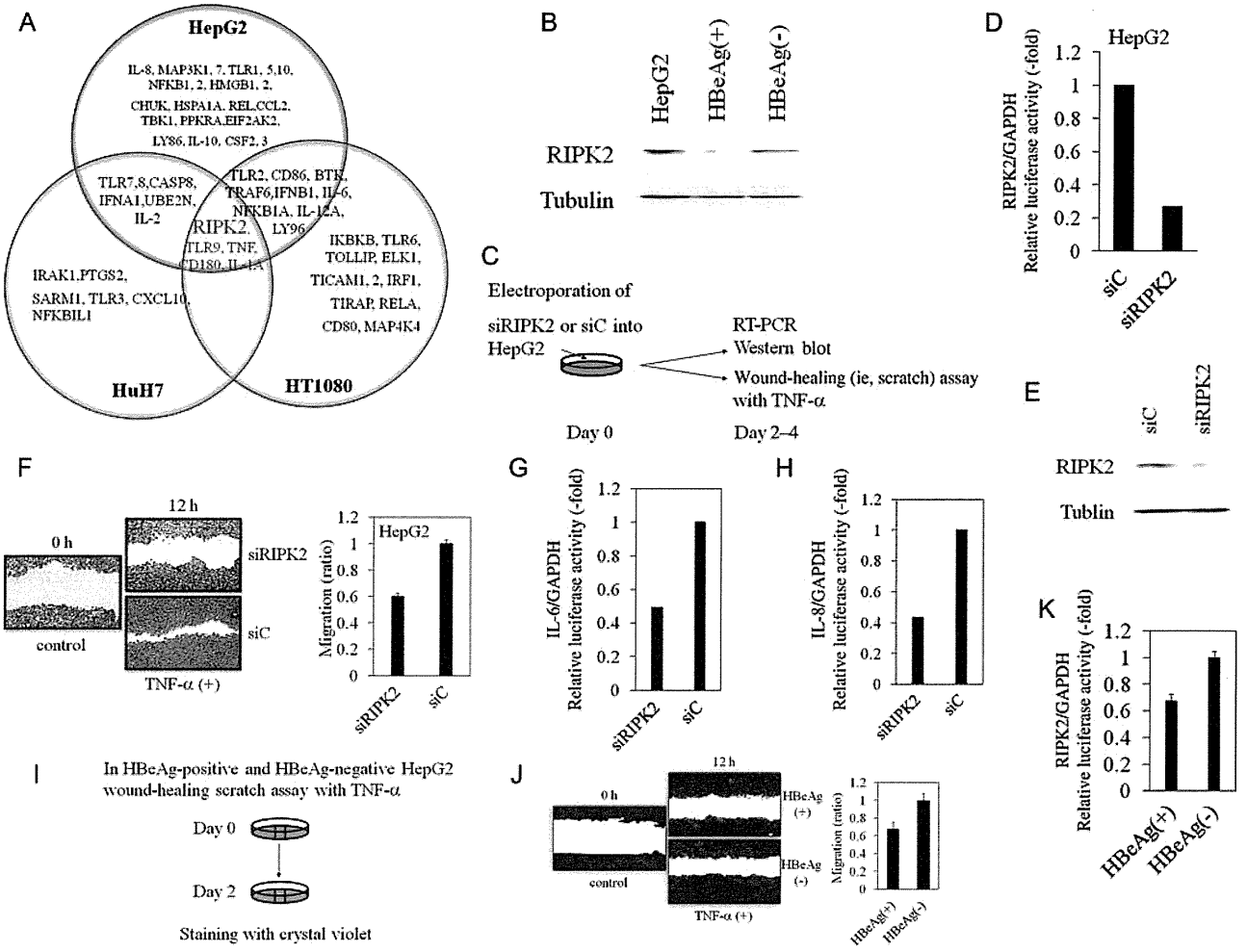

Figure 1. Receptor-interacting serine/threonine protein kinase 2 (RIPK2) expression is downregulated by hepatitis B virus e antigen (HBeAg), and knockdown of RIPK2 and HBeAg impairs hepatic wound repair. *A*, Venn diagram representing Toll-like receptor (TLR)–related genes downregulated ≥1.3-fold in HBeAg-positive HepG2/Huh7/HT1080 cells, compared with HBeAg-negative cells. Cellular RNA was extracted and analyzed with focused array, quantifying 84 genes. Gene expression levels were normalized to actin and GAPDH expression levels. *B*, HBeAg downregulates RIPK2 expression in HepG2 cells. Western blot analysis of RIPK2 and tubulin expression in HepG2, HBeAg(+) HepG2, and HBeAg(−) HepG2. *C*, Experimental protocol of electroporation of control (siC) and RIPK2 (siRIPK2) small interfering RNA (siRNA) into HepG2 cells. *D* and *E*, Real-time polymerase chain reaction (PCR; *D*) and Western blot (*E*) analyses of RIPK2 expression in siC- or siRIPK2-expressing HepG2 cells. RIPK2 messenger RNA (mRNA) levels were normalized to GAPDH levels. *F–H*, siC- and siRIPK2-transfected HepG2 cells were scratch wounded and incubated with 10 ng/mL tumor necrosis factor α (TNF-α), and cell migration was analyzed after 12 hours and quantified using Scion Image (*F*). Interleukin 6 (IL-6; *G*) and interleukin 8 (IL-8; *H*) mRNA expression are quantified by real-time reverse transcription–PCR (RT-PCR) and expressed relative to GAPDH mRNA expression. *I*, Protocol of wound-healing (ie, scratch) assay in HBeAg(+) and HBeAg(−) HepG2 cells. TNF-α was used at 10 ng/mL. *J*, Cell migration was analyzed using Scion Image. *K*, RIPK2 mRNA expression was quantified by real-time RT-PCR and expressed relative to GAPDH mRNA expression. Primers specific for RIPK2 were 5′-AGACAC-TACTGACATCCAAG-3′ (sense) and 5′-CACAAGTATTTCCGGGTAAG-3′ (antisense), and primers for other genes were as described previously [4]. Data are mean values ± SD of 3 independent experiments.

(Figure 1*A*). Western blot analyses confirmed lower levels of RIPK2 in HBeAg-positive HepG2 than in HBe-negative HepG2 or parental HepG2 (Figure 1*B*). The fact that RIPK2 is one of the targets for the ubiquitin proteasome system and uses a ubiquitin-dependent mechanism to achieve NF-κB activation [6] might be a reason for the differences between RIPK2 mRNA and protein expression status. We also observed lower levels of RIPK2 mRNA expression (0.18-fold) in HepG2.2.15 cells, which secrete complete HBV virion and HBeAg, compared with expression in HepG2 cells (data not shown).

Knockdown of RIPK2 and HBeAg Impairs Hepatic Cell Migration

It has recently been reported that RIPK2 expression is induced by TNF-α plus scratch wounding in keratinocytes [10]. Therefore, we next examined whether RIPK2 affected hepatic

wound healing in the presence of TNF-α in vitro (Figure 1*C*). As shown in Figure 1*D* and 1E, RIPK2 mRNA and protein expression were efficiently decreased in HepG2 cells transfected with RIPK2 siRNA (siRIPK2), but not control (siC). RIPK2 silencing reduced hepatic wound closure 1.8-fold, which was associated with a 2-fold decrease in IL-6 production, known to be an important cytokine for the regeneration of liver [11], and a 2.3-fold decrease in interleukin 8 production (Figure 1*F–H*). Importantly, RIPK2 silencing did not affect cell viability (data not shown).

Given that HBeAg downregulates RIPK2 expression (Figure 1*A* and 1*B*), we examined whether HBeAg has an effect on hepatic wound healing in the presence of TNF-α (Figure 1*I*). As expected, we observed that both cell migration

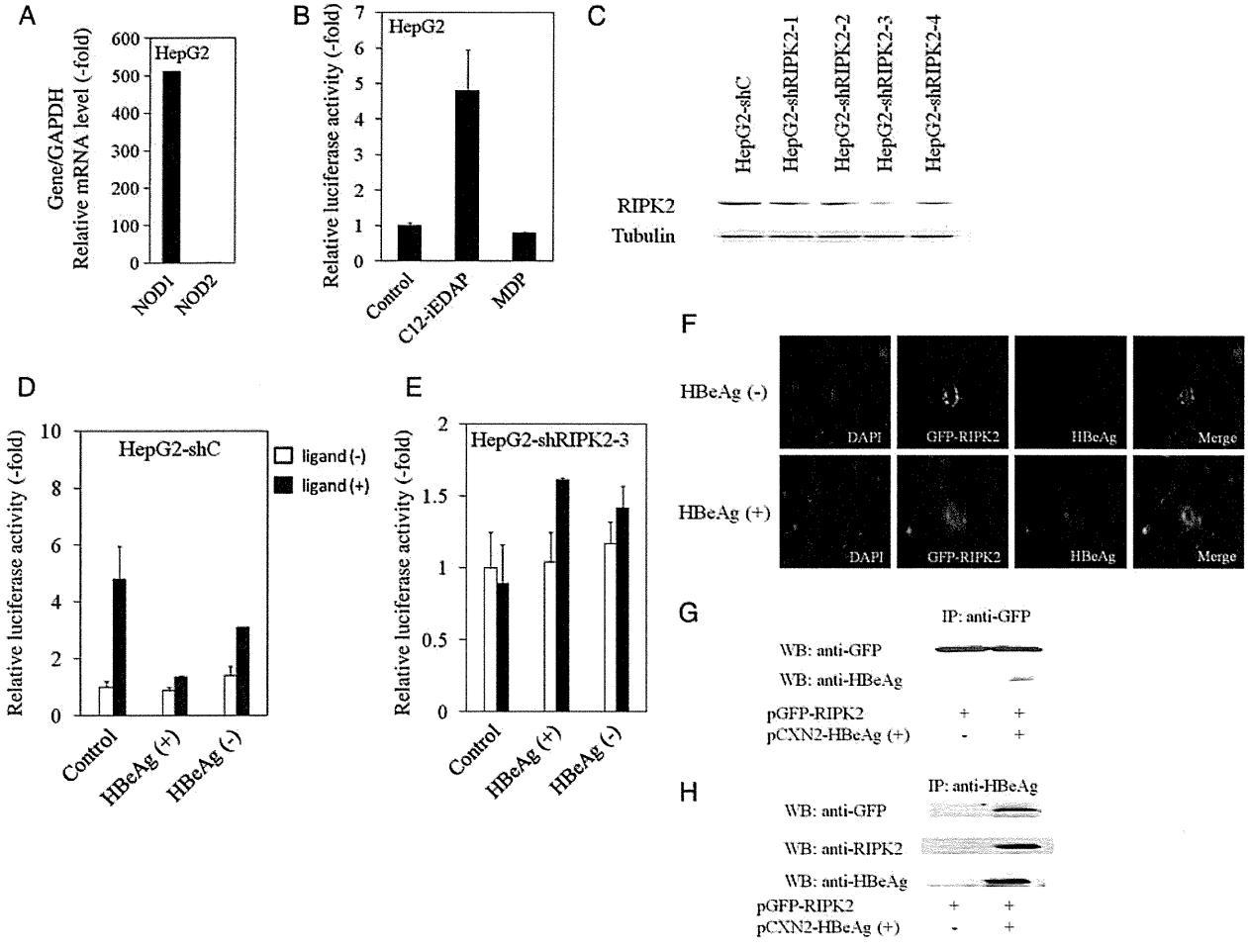

Figure 2. The nucleotide-binding oligomerization domain–containing protein 1 (NOD1) ligand C12-iEDAP induces NF-κB activation, knockdown of receptor-interacting serine/threonine protein kinase 2 (RIPK2) inhibits NOD1 ligand–induced NF-κB activation in HepG2 cells, and hepatitis B virus e antigen (HBeAg) interacts with RIPK2. *A*, Real-time reverse transcription–polymerase chain reaction analysis of NOD1 and NOD2 messenger RNA expression in HepG2. NOD1 and NOD2 expression levels were normalized to GAPDH expression levels. *B*, NF-κB–driven luciferase activity in HepG2 cells stimulated with the NOD1 ligand C12-iEDAP or the NOD2 ligand muramyl dipeptide (MDP) in HepG2. *C*, Western blot analysis of RIPK2 and tubulin expression in HepG2 cells stably transfected with control small hairpin RNA (shRNA; HepG2-shC) or with RIPK2 shRNA (HepG2–shRIPK2-1/2-4) expressing plasmids. *D* and *E*, HepG2-shC (*D*) and HepG2–shRIPK2-3 (*E*) cell lines were transiently transfected with pCXN2, pCXN2-HBeAg(+), or pCXN2-HBeAg(−) plasmids together with pNF-κB–luc. Cells were treated for 4 hours, with or without NOD1 ligand C12-iEDAP (2.5 μg/mL), and luciferase activity was determined. Primers specific for NOD1 (sense primer: 5′-ACTACCTCAAGCTGACCTAC-3′; antisense primer: 5′-CTGGTTTACGCTGAGTCTG-3′), for NOD2 (sense primer: 5′-CCTTGCATGCAGGCAGAAC-3′; antisense primer: 5′-TCTGTTGCCCCAGAATCCC-3′), and for other genes as described previously were purchased from Sigma [4]. *F*, HBeAg specifically colocalizes with RIPK2. COS7 cells were transiently cotransfected with 0.1 μg pCXN2-HBeAg(+) or pCXN2-HBeAg(−) together with 0.3 μg pGFP–human RIPK2. HBeAg was revealed with anti-HBeAg primary antibody and Alexa-Fluor-548 secondary antibody. *G* and *H*, HEK293T cells were transiently transfected with or without GFP-RIPK2 and HBeAg-expressing plasmids. Cellular extracts were precleared with protein G–Sepharose, and interacting complexes were immunoprecipitated (IP) with either anti-GFP (*G*) or anti-HBeAg (*H*) antibodies. Immunocomplexes were separated by sodium dodecyl sulfate–polyacrylamide gel electrophoresis, and proteins were visualized by immunoblotting (WB) with indicated antibodies. Results are representative of 3 independent experiments.

and RIPK2 mRNA expression were reduced in HBeAg-positive HepG2 cells, compared with HBeAg-negative cells (1.5-fold decrease; Figure 1*J* and 1*K*). These results suggest that HBeAg impairs hepatic cell migration–dependent RIPK2 expression. Among NF-κB–targeting genes, expression of vimentin mRNA was impaired in HepG2-shRIP2 and in HBeAg-positive HepG2 (data not shown), and vimentin might be one of the candidates for impairment of their migrations [12].

RIPK2 Plays an Important Role in NF-κB Activation Induced by NOD1 Ligand, and HBeAg Blocks This Pathway

HepG2 cells express NOD1 but not NOD2 at the mRNA level (Figure 2*A*). In agreement with this finding, NF-κB was activated in HepG2 cells exposed to NOD1 ligand C12-iEDAP (level of activation, 4.8-fold, compared with untreated control) but not in those exposed to NOD2 ligand MDP (Figure 2*B*). As for Huh7 cells, activation of NF-κB was not detected following exposure to C12-iEDAP or MDP (data not shown). These results suggest that C12-iEDAP triggered NF-κB activation through NOD1 in HepG2 cells, which is consistent with findings from a previous study [9].

We examined whether knockdown of RIPK2 has an effect on NOD1-induced NF-κB activation in HepG2 cells. First, we established HepG2 cell lines that constitutively expressed RIPK2-shRNA (HepG2-shRIPK2-1/2-4) or control-shRNA (HepG2-shC) (Figure 2*C*). The HepG2–shRIPK2-3 cell line, which expresses the lowest levels of RIPK2, and the HepG2-shC cell line were treated for 4 hours, with or without C12-iE-DAP, before measurement by the NF-κB–driven luciferase assay (Figure 2*D* and 2*E*). C12-iEDAP triggered NF-κB activation in HepG2-shC (Figure 2*D*) but not in HepG2–shRIPK2-3 (Figure 2*E*), indicating that RIPK2 plays an important role in NF-κB activation induced through NOD1 triggering.

To assess the influence of HBeAg in that pathway, we measured NOD1-mediated NF-κB activity in HepG2-shC and HepG2–shRIPK2-3 cell lines transiently transfected with HBeAg-expressing plasmids. As shown in Figure 2*D*, HBeAg expression in HepG2-shC abolished C12-iEDAP–induced NF-κB activation.

HBeAg Interacts With RIPK2 and Colocalizes With RIPK2

RIPK2 mediates activation of transcription factors, such as NF-κB, following its activation, which is initiated by membrane-bound or intracytosolic receptors, such as TLR, NOD1, and NOD2 [7, 13, 14]. Confocal microscopy analysis of cells transfected with GFP-RIPK2 revealed subcellular localization of RIPK2 (data not shown). To compare the localization of RIPK2 with that of HBeAg, cells were cotransfected with pGFP–human RIPK2 with pCXN2-HBeAg(+) or pCXN2-HBeAg(−). After 48 hours, cells were stained with mouse monoclonal anti-HBe antibody. Confocal microscopy suggested subcellular colocalization of RIPK2 with HBeAg (Figure 2*F*). Reinforcing this assumption, GFP-RIPK2 coimmunoprecipitated with HBeAg (Figure 2*G*), while HBeAg coimmunoprecipitated with RIPK2 (Figure 2*H*) in transiently transfected cells with RIPK2- and HBeAg-expressing plasmids.

DISCUSSION

In the present study, we have shown the expression of NOD1 and NOD1 ligand–induced NF-κB activation in HepG2 cells and that RIPK2 plays an important role in NOD1 ligand–induced NF-κB activation. NF-κB activation plays an essential role in the production of inflammatory cytokines such as IL-6, which HBeAg could suppress in hepatocytes [4]. We have also shown that HBeAg inhibits RIPK2 expression and interacts with RIPK2, which may represent 2 mechanisms through which HBeAg blocks NOD1 ligand–induced NF-κB activation, thus contributing to the pathogenesis of chronic HBV infection and establishing viral persistence, although further studies including clinical situations might be needed.

HBeAg can be secreted by hepatocytes. Yet, it has been reported that as much as 80% of the precore protein p22 remains localized to the cytoplasm rather than undergoing further cleavage that allows its secretion as mature HBeAg [15]. Our present study showed subcellular colocalization of HBeAg with RIPK2 (Figure 2*F*). In addition to HBeAg protein in cell culture medium, we observed similar inhibition of NF-κB activation (data not shown).

Overall, we provided a novel molecular mechanism whereby HBeAg modulates innate immune signal-transduction pathways through RIPK2. Elsewhere, it was also reported that HBeAg impairs cytotoxic T-lymphocyte activity [2]. HBeAg inhibits RIPK2 expression and interacts with RIPK2, decreasing NF-κB activation and inflammatory cytokine production in hepatocytes. Taken together, HBeAg could impair both innate and adaptive immune responses to promote chronic HBV infection.

Notes

Acknowledgments. We thank Prof John C. Reed and Prof Junichi Miyazaki, for providing the plasmids, and Ms. Satomi Hasegawa, for providing technical assistance.

Financial support. This work was supported by the Japan Science and Technology Agency, Ministry of Education, Culture, Sports, Science, and Technology, Japan (21590829 to T. K. and 21590828 to F. I.); the Japan Society of Hepatology (T. K.); the Chiba University Young Research-Oriented Faculty Member Development Program in Bioscience Areas (T. K.); and the Research Grant-in-Aid from Miyakawa Memorial Research Foundation (W. S.).

Potential conflicts of interest. All authors: No reported conflicts.

All authors have submitted the ICMJE Form for Disclosure of Potential Conflicts of Interest. Conflicts that the editors consider relevant to the content of the manuscript have been disclosed.

References

1. Ait-Goughoulte M, Lucifora J, Zoulim F, Durantel D. Innate antiviral immune responses to hepatitis B virus. Viruses **2010**; 2:1394–410.
2. Chen M, Sallberg M, Hughes J, et al. Immune tolerance split between hepatitis B virus precore and core proteins. J Virol **2005**; 79:3016–27.
3. Ou JH, Laub O, Rutter WJ. Hepatitis B virus gene function: the precore region targets the core antigen to cellular membranes and causes the secretion of the e antigen. Proc Natl Acad Sci U S A **1986**; 83:1578–82.
4. Wu S, Kanda T, Imazeki F, et al. Hepatitis B virus e antigen down-regulates cytokine production in human hepatoma cell lines. Viral Immunol **2010**; 23:467–76.
5. Lang T, Lo C, Skinner N, Locarnini S, Visvanathan K, Mansell A. The hepatitis B e antigen (HBeAg) targets and suppresses activation of the Toll-like receptor signaling pathway. J Hepatol **2011**; 55:762–9.
6. Hasegawa M, Fujimoto Y, Lucas PC, et al. A critical role of RICK/RIP2 polyubiquitination in Nod-induced NF-kappaB activation. EMBO J **2008**; 27:373–83.
7. Kobayashi K, Inohara N, Hernandez LD, et al. RICK/Rip2/CARDIAK mediates signalling for receptors of the innate and adaptive immune systems. Nature **2002**; 416:194–9.
8. Krieg A, Correa RG, Garrison JB, et al. XIAP mediates NOD signaling via interaction with RIP2. Proc Natl Acad Sci U S A **2009**; 106:14524–9.
9. Scott MJ, Chen C, Sun Q, Billiar TR. Hepatocytes express functional NOD1 and NOD2 receptors: a role for NOD1 in hepatocyte CC and CXC chemokine production. J Hepatol **2010**; 53:693–701.
10. Adams S, Valchanova RS, Munz B. RIP2: a novel player in the regulation of keratinocyte proliferation and cutaneous wound repair? Exp Cell Res **2010**; 316:728–36.
11. Cressman DE, Greenbaum LE, DeAngelis RA, et al. Liver failure and defective hepatocyte regeneration in interleukin-6-deficient mice. Science **1996**; 274:1379–83.
12. Moura-Neto V, Kryszke MH, Li Z, Vicart P, Lilienbaum A, Paulin D. A 28-bp negative element with multiple factor-binding activity controls expression of the vimentin-encoding gene. Gene **1996**; 168:261–6.
13. Meylan E, Tschopp J. The RIP kinases: crucial integrators of cellular stress. Trends Biochem Sci **2005**; 30:151–9.
14. Chin AI, Dempsey PW, Bruhn K, Miller JF, Xu Y, Cheng G. Involvement of receptor-interacting protein 2 in innate and adaptive immune responses. Nature **2002**; 416:190–4.
15. Garcia PD, Ou JH, Rutter WJ, Walter P. Targeting of the hepatitis B virus precore protein to the endoplasmic reticulum membrane: after signal peptide cleavage translocation can be aborted and the product released into the cytoplasm. J Cell Biol **1988**; 106:1093–104.

Journal of Virological Methods xxx (2012) xxx–xxx

Contents lists available at SciVerse ScienceDirect

Journal of Virological Methods

journal homepage: www.elsevier.com/locate/jviromet

Multiplex real-time PCR assays for the detection of group C rotavirus, astrovirus, and Subgenus F adenovirus in stool specimens

Kohji Mori[a,*], Yukinao Hayashi[a], Tetsuya Akiba[a], Miyuki Nagano[a], Tatsuya Tanaka[a], Mitsugu Hosaka[a], Akiko Nakama[a], Akemi Kai[a], Kengo Saito[b], Hiroshi Shirasawa[b]

[a] Department of Microbiology, Tokyo Metropolitan Institute of Public Health, Tokyo 169-0073, Japan
[b] Department of Molecular Virology, Graduate School of Medicine, Chiba University, Chiba, Japan

Article history:
Received 6 June 2012
Received in revised form 24 October 2012
Accepted 30 October 2012
Available online xxx

Keywords:
Gastroenteritis
Real-time PCR
Group C rotavirus
Astrovirus
Subgenus F adenovirus

A B S T R A C T

Group C rotavirus (GCRV), astrovirus (AstV), and adenovirus (subgenus F AdenoV) are etiologic agents of acute nonbacterial gastroenteritis, which often represents community outbreaks. For the efficient detection of GCRV, AstV, and subgenus F AdenoV in stool specimens, a multiplex real-time PCR assay was developed to detect these three viruses simultaneously, with high sensitivity and specificity. In total, 8404 clinical specimens were collected between April 2008 and March 2011 and tested for GCRV, AstV, and subgenus F AdenoV by the multiplex real-time PCR, as well as for norovirus (NoV), sapovirus (SaV), and group A rotavirus (GARV) by non-multiplex real-time PCR. Forty-one specimens were positive for GCRV, AstV, or subgenus F AdenoV, including 15 specimens that were also positive for NoV, SaV, or GARV. Multiple viruses were detected simultaneously in 29 out of 4596 (0.63%) specimens infected with at least one virus. The association rates of AstV and subgenus F AdenoV with other viruses were significantly higher than those of NoV, SaV, GARV, or GCRV.

1. Introduction

Viral gastroenteritis is often caused by norovirus (NoV), sapovirus (SaV), rotaviruses, astrovirus (AstV), and subgenus F adenovirus (AdenoV). NoV and SaV are members of the family *Caliciviridae* and the major causes of epidemic gastroenteritis, whereas viral gastroenteritis caused by group C rotavirus (GCRV), AstV, or subgenus F AdenoV is less frequent. However, community gastroenteritis, the etiologic agents of which should be identified efficiently and correctly, is often caused by GCRV, AstV, and subgenus F AdenoV. Thus, testing methods with high sensitivity for the detection of these three viruses are indispensable.

Rotaviruses are double-stranded RNA viruses belonging to the family *Reoviridae*. Serogroups A, B, and C of the rotaviruses are known to cause gastrointestinal infections in humans. Of these serogroups, serogroup A is the most common worldwide. Group B is considered to be associated solely with epidemic infections, whereas group C rotavirus is associated with gastroenteritis in both sporadic cases and epidemic outbreaks (Gabbay et al., 1999; Hung et al., 1984; Iizuka et al., 2006; Ituriza-Gomara et al., 2000; Jiang et al., 1995; Oishi et al., 1993; Parashar et al., 2003; Sanchez-Fauquier et al., 2003; Sebeta and Steele, 1999; Texeira et al., 1998).

AstV is a single-stranded positive-sense RNA virus belonging to the family *Astroviridae*, which is associated with gastroenteritis in all age groups (Belliot et al., 1997a, 1997b; Blacklow and Greenberg, 1991; Cruz et al., 1992; Herrmann et al., 1988; Lew et al., 1990; Lewis et al., 1989; Madeley and Codgrove, 1975; Midthun et al., 1993; Mitchell et al., 1993, 1995; Oishi et al., 1994; Putzker et al., 2000).

AdenoV is a double-stranded DNA virus belonging to the family *Adenoviridae*, which is classified into six subgenera—A to F (Wadell, 1984). Subgenus F AdenoV (types 40 and 41) includes enteric AdenoV, which causes viral gastroenteritis (Uhnoo et al., 1984), although community gastroenteritis cases caused by AdenoV are less frequent than those caused by other gastroenteritis viruses are (Chiba et al., 1983; Mori et al., 2003).

Diagnostic tests employing molecular methods for the detection of enteric viruses have revealed the role of these viruses in the etiology of sporadic and epidemic gastroenteritis. Reverse transcription (RT)-PCR assays and real-time RT-PCR assays are the primary methods for the detection of NoV and SaV in stool specimens (Kageyama et al., 2003; Kojima et al., 2002; Oka et al., 2006; Okada et al., 2006). RT-PCR, PCR, and commercially available antigen-detection kits, such as the reverse passive hemagglutination test (RPHA) and enzyme immunoassay (EIA), are used routinely for the detection of GCRV, AstV, and subgenus F AdenoV viruses in stool specimens.

* Corresponding author at: Tokyo Metropolitan Institute of Public Health, Department of Microbiology, 3-24-1 Hyakunin-cho, Shinjuku-ku, Tokyo 169-0073, Japan. Tel.: +81 3 3363 3231; fax: +81 3 3363 3263.
E-mail address: Kouji_Mori@member.metro.tokyo.jp (K. Mori).

0166-0934/$ – see front matter © 2012 Elsevier B.V. All rights reserved.
http://dx.doi.org/10.1016/j.jviromet.2012.10.019

Although assays using antigen-detection kits are simpler to perform and highly specific, the sensitivity of such kits is often too low for the direct detection of viral antigens in stool specimens (Belliot et al., 1997b; Jiang et al., 1995; Logan et al., 2006b).

Real-time PCR assays enable increased detection rates of causative agents of gastroenteritis compared with the detection rates estimated by antigen-detection assays (Gunson et al., 2003; Pang et al., 1999). The aim of this study was to develop a multiplex real-time PCR assay with high sensitivity and specificity for the efficient and reliable detection of GCRV, AstV, and subgenus F AdenoV in clinical stool specimens.

2. Materials and methods

2.1. Specimens

Stool specimens collected from 8404 gastroenteritis patients in Tokyo, Japan, between April 2008 and March 2011 were kept at −80 °C until analysis. The specimens were homogenized in phosphate-buffered saline (PBS) as 10% homogenates before testing, and stored at 4 °C.

2.2. Detection of viral antigen using commercial kits

For detection of viral antigens, an RPHA test kit for GCRV (Denka Seiken, Tokyo, Japan), an EIA kit for AstV (Amplified IDEIA Astrovirus, Oxoid, Hampshire, UK), and an EIA kit for subgenus F AdenoV (Premier Adenoclone, Cambridge Biotech, Cambridge, UK) were used according to the manufacturer's instructions.

2.3. Nucleic acid extraction and reverse transcription

Samples (10% homogenates) were centrifuged at 2000 × *g* for 5 min at 4 °C, and the supernatants were centrifuged at 7200 × *g* for 30 min at 4 °C. For polyethylene glycol (PEG) precipitation, the supernatant of each sample was suspended in a solution containing 8% PEG6000 and 0.4 M NaCl, and incubated overnight at 4 °C. The precipitated virus was recovered by centrifugation at 11,000 × *g* for 30 min, and the concentrated virus was resuspended in 100 μl of PBS for viral RNA and DNA extraction.

The concentrated samples were incubated in a buffer with 100 μg/ml of proteinase K for 30 min at 37 °C, and then, 100 μl of 4 M NaCl and 100 μl of 10% cetyltrimethyl ammonium bromide (CTAB) were added to the buffer. After incubation for 30 min at 56 °C, the samples were extracted in a phenol-chloroform–isoamyl alcohol mixture (25:24:1) with vortexing, and then centrifuged at 13,000 × *g* for 15 min. Viral RNA and DNA in the upper phase were precipitated by addition of 750 μl of ethanol with 1 mg of glycogen and 30 μl of 3 M sodium acetate and by incubation of the mixture at −80 °C for 1 h, followed by centrifugation at 13,000 × *g* for 30 min. The pellet was then air-dried and resuspended in 50 μl of distilled water.

For reverse transcription, 12 μl of the sample was added to 17.5 μl of the reagent mix, including 1 mM of each deoxynucleoside triphosphate (dNTP), 10 mM of dithiothreitol (DTT), 30 U of an RNAse inhibitor, 75 pmol of random hexamers, and 0.5 μl (200 U) of M-MLV reverse transcriptase. Reactions were incubated at 42 °C for 1 h.

2.4. Real-time PCR primer and probe design

Sequences from highly conserved target genes were used for the design of real-time PCR assays, as outlined in Table 1. GenBank accession numbers (ID) of sequences used are as follows: ROTGP8A, AY392447, AM118023, X77256, X77257, RGU20992, AB086962, AF323982, AB086966, AB086968, AB086969, X77258, AF120478, AF225552, AY803726, and EF528571 for GCRV; Z25771, AY720892, NC_001943, and ATVPOLY6A for AstV type 1; HUANSSPS for AstV type 2; AF141381 and AF292074 for AstV type 3; AY720891, DQ070852, DQ344027, and AF292075 for AstV type 4; DQ028633 and AF292076 for AstV type 5; AF292077 for AstV type 6; AF248738 for AstV type 7; AF260508 for AstV type 8; NC_001454 for subgenus F AdenoV type 40; and DQ315364 for subgenus F AdenoV type 41.

All primers and probes were designed using Primer Express, obtained from Life Technologies (Carlsbad, CA, USA). For the detection of GCRV, CRV7F/R primers and a FAM-labeled CRV7 linear TAMRA probe were designed to target the highly conserved VP7 gene. For AstV, AstF/R primers and a TET-labeled Ast linear TAMRA probe targeting the ORF1b (polymerase) region were designed. For the detection of subgenus F AdenoV, the hexon region was targeted. AdhF/AdFhR primers and a VIC-labeled Adh linear MGB probe were used for the detection of subgenus F AdenoV DNA. A universal primer for subgenera C and F AdenoV, AdhF (Table 1), was designed as the forward primer used for amplifying a synthesized DNA standard for AdenoV.

2.5. Real-time PCR

After reverse transcription, 5 μl of the cDNA or DNA was used as a template for real-time PCR. For multiplex real-time PCR, the template was added to the reaction mixture (TaqMan Universal PCR Master Mix, Life Technologies) containing 40 pmol/μl and 5 pmol/μl of each of the virus-specific primer sets and probes designed for GCRV, AstV, and subgenus F AdenoV. For non-multiplex real-time PCR, the cDNA or DNA was added to the reaction mixture containing 40 pmol/μl of a single primer set and 5 pmol/μl of a single probe, both specific to only a single virus. The real-time PCR was carried out using the Sequence Detection System ABI PRISM 7900HT (Life Technologies) under the following conditions: a 10-min denaturation step at 96 °C and 45 cycles of 96 °C for 15 s and 58 °C for 1 min.

NoV, SaV, and group A rotavirus (GARV) were detected by real-time PCR assays using COG1F/1R and 2F/2R primer pairs and RING1TP and 2TP probes for NoV (Kageyama et al., 2003); SaV124F, 1F, and 5F/1245R primers and SaV124TP and 5TP probes for SaV (Oka et al., 2006); and a JVKF/R primer pair and JVKP probe for GARV (Jothikumar et al., 2009).

2.6. Sequencing analysis

The detected GCRV, AstV, and subgenus F AdenoV were confirmed by conventional RT-PCR or PCR assays (Allard et al., 1990; Belliot et al., 1997b; Gouvea et al., 1991) and sequencing analysis using the dye-terminator method. Conventional PCR-positive samples were purified using NucleoSpin Extract II (MACHEREY-NAGEL, Duren, Germany) and analyzed using a BigDye Terminator v1.1 Cycle Sequencing kit (Life Technologies). The sequences collected were aligned with deposited sequences in the DDBJ/GenBank/EMBL database at the DDBJ BLAST site (http://blast.ddbj.nig.ac.jp/top-j.html).

3. Results

3.1. PCR reaction sensitivity and detection limits

GCRV, AstV, and subgenus F AdenoV were detected successfully by multiplex real-time PCR. To examine the sensitivity and detection limits of the PCR reaction, synthesized DNA standards (FASMAC, Atsugi, Japan) were tested for amplification using real-time PCR assays. The detection limits and amplification efficiencies of the real-time PCR assays were evaluated by amplifying duplicate aliquots of 10-fold dilutions of each synthesized DNA standard.

Please cite this article in press as: Mori, K., et al., Multiplex real-time PCR assays for the detection of group C rotavirus, astrovirus, and Subgenus F adenovirus in stool specimens. J. Virol. Methods (2012), http://dx.doi.org/10.1016/j.jviromet.2012.10.019

Table 1
Primers and probes designed for real-time PCR assays of group C rotavirus, astrovirus, and subgenus F adenovirus.

Viruses (Target gene)	Primer/probe (5′label-3′label)	Sequence[a] (5′-3′)	Position[b]
Group C rotavirus (VP7)	CRV7F	gCTgCATTTggTAgTgACTgYgA	616–638
	CRV7R	AgTTTCTgTACTAgCCggTgAACA	682–705
	CRV7 (FAM-TAMRA)	TCTgTCTgTCCATTAgATACTACAAgTAATggAATYgg	642–680
Astrovirus (Polymerase)	AstF	CATgggAAgCTCCTRTgCTAYCA	4144–4167
	AstR	gABAggCAgTgYTCYACA	4213–4230
	Ast (TET-TAMRA)	TgCTYgCTgCRTTYATggCAgARg	4169–4193
Subgenus F adenovirus (Hexon)	AdhF	CAggACgCCTCggAgTAA	17649–17666
	AdFhR	CCAgCgTAAAgCgCACTT	17839–17856
	AdChR	TCTAAACTTgTTATTCAggCTgAAg	17711–17735
	Adh (VIC-MGB)	TTYgCCCgYgCCAC	17688–17701

[a] Mixed bases in degenerate primers and probes are as follows: Y = C/T, R = A/G, and B = G/C/T.
[b] The position of each primer is the nucleotide number of the following gene sequences: GenBank ID: X77258 (Preston strain) for group C rotavirus; GenBank ID: ATVPOLY6A (OX1 strain) for astrovirus; and GenBank ID: DQ315364 (Tak strain) for adenovirus.

Because the synthesized DNA of AdenoV was too short for amplification by the AdhF/AdFhR primers, AdChR was used as the reverse primer instead of AdFhR. Five specimens positive for subgenus F AdenoV were tested using real-time PCR assays with the AdhF/AdFhR or AdhF/AdChR primer pairs. No significant difference was observed in the threshold cycle (Ct) values between the primer pairs ($p = 0.469$) for subgenus F AdenoV detection (data not shown). The detection limit of the AdFhR primer was determined to be comparable to that of AdChR.

For strains OX3, OX4, OX5, OX6, and OX7 of AstV, amplification products generated from diluted synthesized DNA standards using the AstF/R primer pair and Ast probe showed a linear relationship in the range of 5×10^0 to 5×10^5 copies per assay; the same results were produced from standards for the Tak strain of subgenus F AdenoV by using the AdhF/AdChR primer pair and Adh probe. A linear relationship in the range of 5×10^1 to 5×10^5 copies per assay was observed for diluted DNA standards of the Preston strain of GCRV by using the CRV7F/7R primer pair and CRV7 probe, as well as for the strains OX1, OX2, and Yuc-8 of AstV by using the AstF/R primer pair and Ast probe (Fig. 1).

3.2. Detection limits of real-time PCR and antigen-detection kits

To evaluate the performance of the multiplex real-time PCR assays for GCRV, AstV, and subgenus F AdenoV compared to the performance of commercially available antigen-detection kits, six GCRV-, six AstV-, and four subgenus F AdenoV-positive specimens collected before March 2008 were diluted serially, from which nucleic acids were extracted and used to examine detection limits. As shown in Table 2, the detection limits of GCRV by using RPHA ranged from 4-fold to 16-fold dilutions, and from 80-fold to 320-fold dilutions by using real-time PCR without the heat-denaturing step before the RT reaction. The detection limit for AstV by using EIA ranged from 0-fold to 10-fold dilutions. In contrast, AstV was detectable in 320-fold dilutions of the six samples by using real-time PCR, including two samples that tested negative using EIA. The detection limit of subgenus F AdenoV ranged from 0-fold to 160-fold dilutions by using EIA, and was 320-fold dilution by using real-time PCR. The detection limits of the real-time PCR assays for GCRV, AstV, and subgenus F AdenoV were lower than those of commercially available antigen-detection kits. These results were consistent with those of previous studies comparing PCR and antigen-detection methods, which reported significantly increased detection rates for PCR (Gunson et al., 2003; Higuchi et al., 1993; Jothikumar et al., 2009; Kageyama et al., 2003; Logan et al., 2006a; Mackay et al., 2002; Oka et al., 2006; Pang et al., 1999; Royuela et al., 2006; Wittman et al., 1997).

3.3. Multiplex real-time PCR

The performance of a multiplex real-time PCR assay for the simultaneous detection of multiple viruses was tested by comparing this assay to virus-specific non-multiplex real-time PCR assays designed for GCRV, AstV, and subgenus F AdenoV. The same specimens used for the comparison of PCR and antigen-detection methods were screened using a non-multiplex real-time PCR with a single primer pair and probe.

As shown in Fig. 2, no significant differences were observed in the Ct values generated using non-multiplex PCR and multiplex PCR ($p = 0.948$). However, significant differences were observed in Ct values observed for GCRV detection assays between samples subjected to the heat-denaturing process and those that were not denatured ($p < 0.001$; Fig. 2). This improvement in sensitivity for GCRV detection using the denaturing process might be due to tight binding of double-stranded RNA, as observed in a study on RT-PCR GARV detection (Gouvea et al., 1990).

3.4. Detection of GCRV, AstV, and subgenus F AdenoV in specimens

The 8404 clinical specimens collected between April 2008 and March 2011 were tested for NoV, SaV, and GARV by using non-multiplex real-time PCR. As shown in Table 3, 4570 (54.4%) of the 8404 specimens were positive for NoV, SaV, and GARV. Ten specimens were infected with more than one of these viruses. To evaluate the specificity and sensitivity of multiplex real-time PCR

Table 2
Detection limits of a commercial antigen-detection kit and real-time PCR for group C rotavirus, astrovirus, and subgenus F adenovirus from stool specimens.

	Samples	Antigen detection kit	Real-time PCR[a]
Group C rotavirus	a	×16	×320
	b	×4	×160
	c	×16	×320
	d	×4	×160
	e	×16	×320
	f	×16	×80
Astrovirus	a	N.D.	×320
	b	×10	×320
	c	×1	×320
	d	×1	×320
	e	N.D.	×320
	f	×10	×320
Subgenus F adenovirus	a	×1	×320
	b	×1	×320
	c	×160	×320
	d	×40	×320

N.D.: not detected.
[a] Without the denaturation step before the RT reaction.

Please cite this article in press as: Mori, K., et al., Multiplex real-time PCR assays for the detection of group C rotavirus, astrovirus, and Subgenus F adenovirus in stool specimens. J. Virol. Methods (2012), http://dx.doi.org/10.1016/j.jviromet.2012.10.019

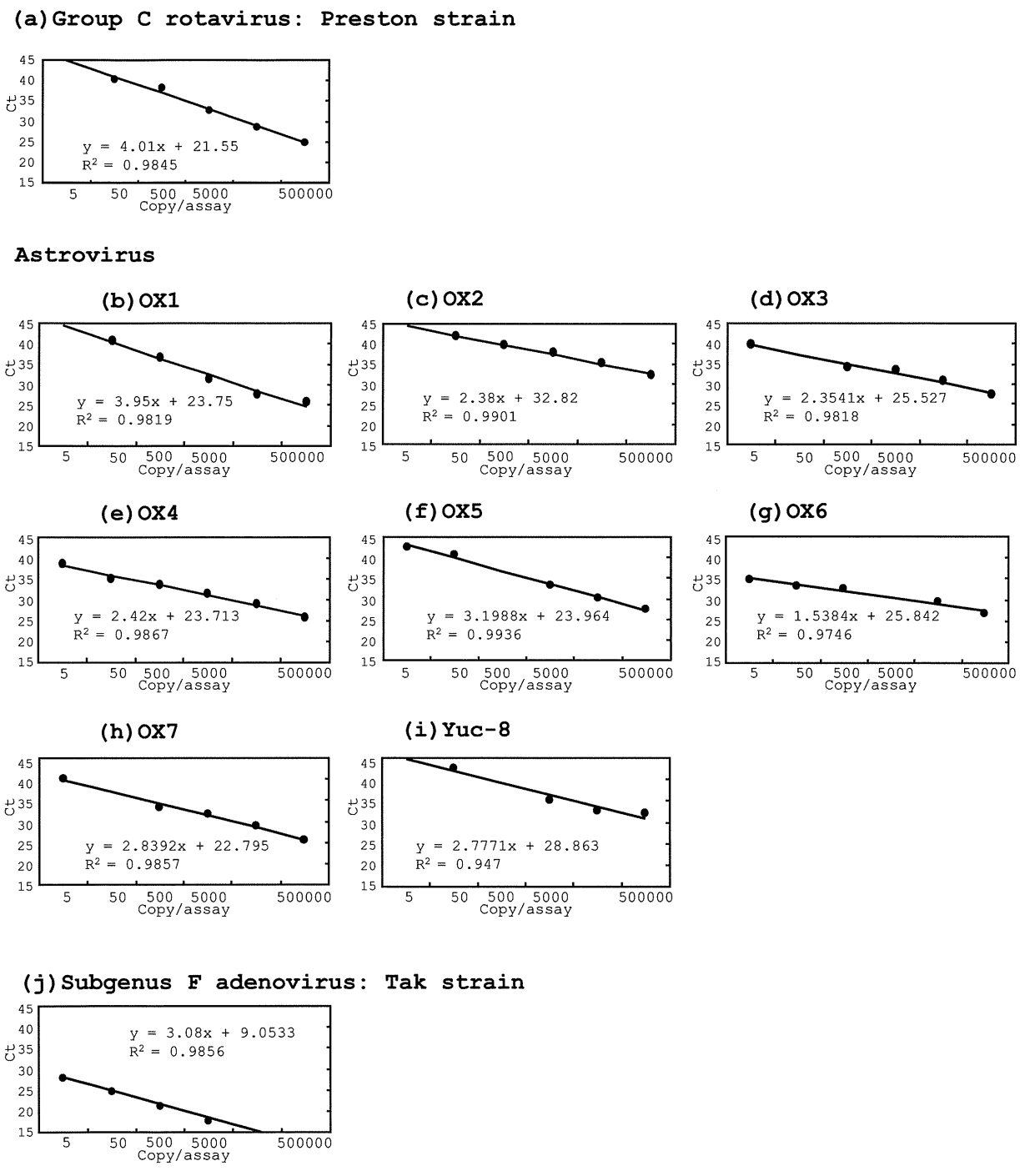

Fig. 1. Amplification of 10-fold serially diluted synthesized DNA templates by real-time quantitative RT-PCR with a single primer pair and probe for group C rotavirus strain Preston (a); astrovirus strains OX1 (b), OX2 (c), OX3 (d), OX4 (e), OX5 (f), OX6 (g), OX7 (h), and Yuc-8 (i); and subgenus F adenovirus strain Tak (j). The C_t values were plotted with the standard curve as indicated.

for the detection of GCRV, AstV, and subgenus F AdenoV, all 8404 specimens were screened using multiplex real-time PCR. Forty-one specimens were positive for GCRV, AstV, or subgenus F AdenoV, including those from 37 patients infected with only a single virus and those from four patients who were infected by more than one virus. Fifteen SaV-, NoV-, or GARV-positive specimens were also positive for GCRV, AstV, or subgenus F AdenoV (Table 3). From this screen, 4596 specimens (54.7%) were found to be positive for NoV, SaV, GARV, GCRV, AstV, or subgenus F AdenoV, totaling 4625 infections. As shown in Table 4, 4387 of NoV (94.9%), 156 of SaV (3.37%), 37 of GARV (0.80%), six of GCRV (0.13%), 31 of AstV (0.67%), and eight of subgenus F AdenoV (0.17%) positive specimens were detected out of the 4596 specimens. The detection rate for NoV was significantly higher ($p < 0.001$) than that for SaV, GARV, GCRV, AstV, and subgenus F AdenoV. Multiple viruses were detected simultaneously in 29 out of 4596 virus-detected specimens (0.63%). The

Please cite this article in press as: Mori, K., et al., Multiplex real-time PCR assays for the detection of group C rotavirus, astrovirus, and Subgenus F adenovirus in stool specimens. J. Virol. Methods (2012), http://dx.doi.org/10.1016/j.jviromet.2012.10.019

Table 3
Detection of gastroenteritis viruses by real-time PCR.

Specimens	Numbers of specimens (%)		
Specimens positive for gastroenteritis viruses tested	4596(54.7)		
SaV-, NoV-, GARV-positives		4570(54.4)[a]	
Single infection			4560(54.3)[a]
Double infection			10(0.1)
GCRV-, AstV-, AdenoV-positives		41(0.49)[b]	
Single infection			37(0.44)[b]
Double infection			4(0.05)
Specimens negative for gastroenteritis viruses tested	3808(45.3)		
Total	8404(100)		

[a] Fifteen specimens positive for GCRV, AstV, or subgenus F AdenoV are included.
[b] Fifteen specimens positive for SaV, NoV, or GARV are included.

simultaneous detection of viruses in these specimens was not due to cross-reaction, as the presence of multiple viruses was confirmed by targeted sequencing of amplified viral genomes (data not shown). Nineteen cases of NoV, twelve cases of SaV, four cases of GARV, one case of GCRV, sixteen cases of AstV, and six cases of subgenus F AdenoV were associated with other viruses (Table 4). All of these 29 specimens in which multiple viruses were detected simultaneously were infected with two different viruses. As shown in Table 4, the association rates of AstV (16/31, 51.6%) and subgenus F AdenoV (6/8, 75.0%) with other viruses were significantly higher ($p = 0.004$ and $p < 0.001$, respectively) than those of NoV (19/4387, 0.43%), SaV (12/156, 7.69%), GARV (4/37, 10.8%), and GCRV (1/6, 16.7%).

4. Discussion

Various agents, such as NoV, SaV, GARV, GCRV, AstV, and subgenus F AdenoV, cause viral gastroenteritis. To identify the viruses underlying community gastroenteritis outbreaks, effective screening for strains other than the major causal virus, NoV, is required. With this goal in mind, a multiplex real-time TagMan PCR assay was developed for the detection of GCRV, AstV, and subgenus F AdenoV in stool specimens by using newly designed primer pairs and probes.

Various molecular techniques have been developed for the detection of gastroenteritis viruses in stool specimens with high sensitivity and specificity (O'Neill et al., 2002; Pring-Akerblom et al., 1997; Sen et al., 2000; Uhnoo et al., 1984). Of these methods, RT-PCR and PCR assays are known to have higher sensitivity than other commonly used approaches, such as commercial viral antigen-detection kits and electron microscopy-based observation of viral particles (Gunson et al., 2003; Pang et al., 1999). Although the sensitivity of conventional PCR is sufficiently high for the detection of viruses, stool specimens may contain unknown templates that could possibly result in nonspecific amplification; thus, the use of PCR for virus detection requires the design of virus-specific assays (Lamothe et al., 2003).

Real-time RT-PCR and real-time PCR have been reported to be effective methods for the rapid and specific detection of viral pathogens from clinical specimens (Higuchi et al., 1993; Jothikumar et al., 2009; Kageyama et al., 2003; Logan et al., 2006a; Mackay et al., 2002; Oka et al., 2006; Royuela et al., 2006; Wittman et al., 1997). The real-time PCR assays developed in this study were able to detect the presence of virus by using synthesized DNA standards containing only 5–50 copies, exhibiting higher sensitivity than that reported previously for other detection methods such as RPHA or EIA. Although the cost of real-time PCR assays is much greater than that of antigen-detection kits, the overall cost is reduced because multiplex reactions allow for the simultaneous detection of GCRV, AstV, and subgenus F AdenoV. Significant differences in the sensitivity were not observed between multiplex real-time PCR and non-multiplex real-time PCR assays for the detection of GCRV, AstV, and subgenus F AdenoV. The specificity of the real-time PCR assays was confirmed by conventional PCR and sequencing analysis of specimens determined to be positive for viruses by using real-time PCR.

NoV is the major cause of epidemic gastroenteritis. Many variants of the virus have been reported, and genotypic and sequence analyses have revealed signatures of rapid evolution (Bok et al., 2009; Bull et al., 2006; Colomba et al., 2007; Lindell et al., 2005; Lopman et al., 2004). In this study, NoV was detected in 4387 (94.9%) out of the 4596 stool specimens positive for the examined viruses, and the detection rate of NoV in gastroenteritis cases was much higher than that of SaV, GARV, GCRV, AstV, and subgenus F AdenoV.

However, viral gastroenteritis is often caused by simultaneous infection with multiple viruses. Cases of patients infected simultaneously with AstV and other viruses, including patients infected with three viral agents, have been reported previously (Colomba et al., 2007; Harada et al., 2009; Noel and Cubitt, 1994; Taylor et al., 1997). Therefore, to understand the distribution of gastroenteritis pathogens in clinical specimens, it is necessary to screen patients for the presence of all viruses. Compared to individual virus-specific real-time RT-PCR assays, the multiplex real-time PCR assays developed in this study for the simultaneous detection of GCRV, AstV, and subgenus F AdenoV in clinical stool specimens showed no decreased sensitivity. Thus, the application of this method to viral testing would facilitate effective detection of GCRV, AstV, and subgenus F AdenoV.

Twenty-nine specimens of patients with gastroenteritis screened in this study were found to be infected with more than one virus. The sensitivity of real-time PCR is so high that the viral passage should be considered, especially in cases of simultaneous

Table 4
Prevalence of norovirus and other gastroenteritis viruses detected simultaneously in stool specimens by real-time RT-PCR.

Simultaneously detected virus	Detected viruses						
	NoV	SaV	GARV	GCRV	AstV	SF AdenoV	Total
None	4368(94.4%)	144(3.11%)	33(0.71%)	5(0.11%)	15(0.32%)	2(0.04%)	4567(98.7%)
NoV	–	8(0.17%)	1(0.02%)	1(0.02%)	7(0.15%)	2(0.04%)	19(0.41%)
SaV	8(0.17%)	–	1(0.02%)	0	3(0.06%)	0	12(0.26%)
GARV	1(0.02%)	1(0.02%)	–	0	2(0.04%)	0	4(0.07%)
GCRV	1(0.02%)	0	0	–	0	0	1(0.02%)
AstV	7(0.15%)	3(0.06%)	2(0.04%)	0	–	4(0.09%)	16(0.34%)
SF AdenoV	2(0.04%)	0	0	0	4(0.09%)	–	6(0.13%)
Total	4387(94.9%)	156(3.37%)	37(0.80%)	6(0.13%)	31(0.67%)	8(0.17%)	4625(100.0%)

NoV: norovirus; SaV: sapovirus; GARV: group A rotavirus; GCRV: group C rotavirus; AstV: astrovirus; SF AdenoV: subgenus F adenovirus.

Please cite this article in press as: Mori, K., et al., Multiplex real-time PCR assays for the detection of group C rotavirus, astrovirus, and Subgenus F adenovirus in stool specimens. J. Virol. Methods (2012), http://dx.doi.org/10.1016/j.jviromet.2012.10.019

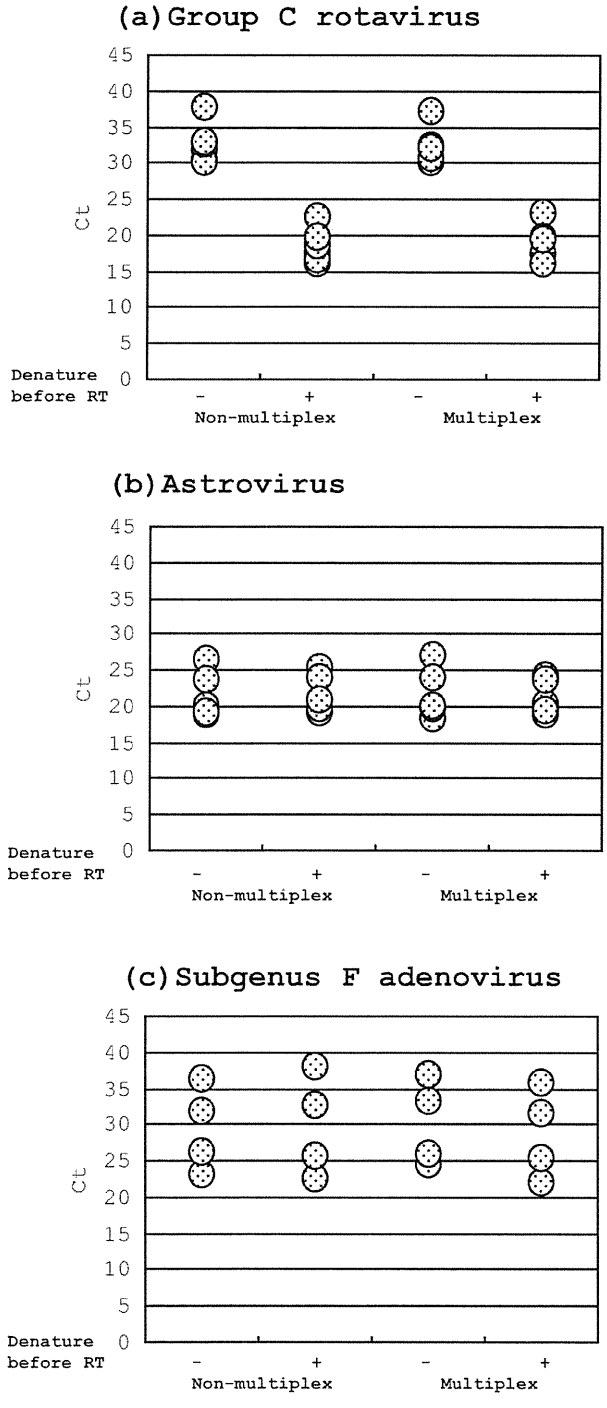

Fig. 2. C_t values of non-multiplex and multiplex real-time RT-PCR assays, with or without a heat-denaturing step before the RT reaction. –, without a denaturing step; +, with a heat-denaturing step at 94 °C for 5 min and chilled on ice before the RT reaction. (+) C_t values for group C rotavirus (a), astrovirus (b), and adenovirus (c) were plotted as indicated.

viral detection. However, the rate of mixed infection in this study was 0.63%, which is relatively low compared to that reported by others (5.2–19.6%; Colomba et al., 2007; Harada et al., 2009). In this study, multiple infection rates of AstV or subgenus F AdenoV with other viruses were significantly higher, highlighting the potential risks of underestimating AstV or subgenus F AdenoV infection.

5. Conclusions

The real-time multiplex PCR assays designed in this study could detect GCRV, AstV, and subgenus F AdenoV in stool samples with high sensitivity and specificity. Significant differences in assay sensitivity were not observed between multiplex real-time PCR and non-multiplex real-time PCR assays. The use of this multiplex real-time PCR assay for GCRV, AstV, and subgenus F AdenoV detection in stool specimens from patients with gastroenteritis would ensure the comprehensive detection of these three viruses, including mixed infections, and could potentially improve understanding of the underlying causative agents of the disease.

References

Allard, A., Girones, R., Juto, P., Wadell, G., 1990. Polymerace chain reaction for detection of adenoviruses in stool samples. J. Clin. Microbiol. 28, 2859–2867.
Belliot, G., Laveran, H., Monroe, S.S., 1997a. Outbreak of gastroenteritis in military recruits associated with serotype 3 astrovirus infection. J. Med. Virol. 51, 101–106.
Belliot, G., Laveran, H., Monroe, S.S., 1997b. Detection and genetic differentiation of human astroviruses: phylogenetic grouping varies by coding region. Arch. Virol. 142, 1323–1334.
Blacklow, N.R., Greenberg, H.B., 1991. Viral gastroenteritis. N. Engl. J. Med. 325, 252–264.
Bok, K., Abente, J.E., Realpe-Quintero, M., Mitra, T., Sosnovstv, V.S., Kapikian, Z.A., Green, Y.K., 2009. Evolutionary dynamics of GII.4 Noroviruses over a 34-years period. J. Virol. 83, 11890–11901.
Bull, R.A., Tu, E.T.V., McIver, C.J., Rawlinson, W.D., White, P.A., 2006. Emergence of a new noroviurs genotype II. 4 variant associated with global outbreaks of gastroenteritis. J. Clin. Microbiol. 44, 327–333.
Chiba, S., Nakata, S., Nakamura, I., Taniguchi, K., Urasawa, S., Fujinaga, K., Nakao, T., 1983. Outbreak of infantile gastroenteritis due to type 40 Adenovirus. Lancet, 954–955.
Colomba, C., Saporito, L., Giammanco, G.M., Grazia, S.D., Ramirez, S., Arista, S., Titone, L., 2007. Norovirus and gastroenteritis in hospitalized children, Italy. EID J. 13, 1389–1391.
Cruz, J.R., Bartlatt, A.V., Herrmann, J.E., Caceres, P., Blacklow, N.R., Cano, F., 1992. Astrovirus associated diarrhea among Gutemalan ambulatory rural children. J. Clin. Microbiol. 30, 1140–1144.
Gabbay, Y.B., Jiang, B., Oliveria, C.S., Mascarenhas, J.D., Leite, J.P., Glass, R.I., Linhares, A.C., 1999. An outbreak of group C rotavirus gastroenteritis among children attending a day-care centre in Belem, Brazil. J. Diarrhoeal Dis. Res. 17, 69–74.
Gouvea, V., Glass, I.R., Woods, P., Taniguchi, K., Clark, F.H., Forester, B., Fang, Z.Y., 1990. Polymerase chain reaction amplification and typing of rotavirus nucleic acid from stool specimens. J. Clin. Microbiol. 28, 276–282.
Gouvea, V., Allen, R.J., Glass, I.R., Fang, Z.Y., Bremont, M., Cohen, J., McRaeam, A.M., Saif, J.L., Sinarachatanant, P., Caul, E.O., 1991. Detection of group B and group C rotavirus by polymerase chain reaction. J. Clin. Microbiol. 29, 518–523.
Gunson, R.N., Miller, J., Leonard, A., Carman, W.F., 2003. Importance of PCR in the diagnosis and understanding of rotavirus illness in the community. Commun. Dis. Public Health 6, 63–65.
Harada, S., Okada, M., Yahiro, S., Nishimura, K., Matsuo, S., Miyasaka, J., Nakashima, R., Shimada, Y., Ueno, T., Ikezawa, S., Shinozaki, K., Katayama, K., Wakita, T., Takeda, N., Oka, T., 2009. Surveillance of pathogens in outpatients with gastroenteritis and characterization of sapovirus strains between 2002 and 2007 in Kumamoto prefecture, Japan. J. Med. Virol. 81, 1117–1127.
Herrmann, J.E., Blacklow, N.R., Perron-Henry, D.M., Clements, E., Taylor, D.N., Echeverria, P., 1988. Incidence of entric adenoviruses among children in Thailand and significance of these viruses in gastroenteritis. J. Clin. Microviol. 26, 1783–1786.
Higuchi, R., Focker, C., Dollinger, G., Watson, R., 1993. Kinetic PCR analysis: real-time monitoring of DNA amplification reactions. Biotechnology 11, 1026–1030.
Hung, T., Chen, G.M., Wang, C.G., Yao, H.L., Fang, Z.Y., Chao, T.X., Chou, Z.Y., Ye, W., Chang, X.J., Den, S.S., 1984. Waterborne outbreak of rotavirus diarrhea in adults in China caused by a novel rotavirus. Lancet, 1139–1142.
Iizuka, S., Tabara, K., Kawamukai, A., Itogawa, H., Hoshina, K., 2006. An outbreak of group C rotavirus infection in an elementary school in Shimane prefecture, Japan, February 2006. Jpn. J. Infect. Dis. 59, 350–351.
Ituriza-Gomara, M., Green, J., Brown, D.W., Ramsay, M., Desselberger, U., Gray, J.J., 2000. Molecular epidemiology of human group A rotavirus infection in the United Kingdom between 1995 and 1998. J. Clin. Micrbiol. 38, 4394–4401.
Jiang, B., Denneby, P.H., Spangenberger, S., Gentsch, J.R., Glass, R.I., 1995. First detection of group C rotavirus in fecal specimens of children with diarrhea in the United States. J. Infect. Dis. 172, 45–50.
Jothikumar, N., Kang, G., Hill, V.R., 2009. Broadly reactive TaqMan assay for real-time RT-PCR detection of rotavirus in clinical and environmental samples. J. Virol. Method. 155, 126–131.
Kageyama, T., Kojima, S., Shinohara, M., Uchida, K., Fukushi, S., Hoshino, F.B., Takeda, N., Katayama, K., 2003. Broadly reactive and highly sensitive assay for Norwalk-like viruses based on real-time quantitative reverse transcription-PCR. J. Clin. Microbiol. 41, 1548–1557.

Please cite this article in press as: Mori, K., et al., Multiplex real-time PCR assays for the detection of group C rotavirus, astrovirus, and Subgenus F adenovirus in stool specimens. J. Virol. Methods (2012), http://dx.doi.org/10.1016/j.jviromet.2012.10.019

Kojima, S., Kageyama, T., Fukushi, S., Hoshino, F.B., Shinohara, M., Uchida, K., Natori, K., Takeda, N., Katayama, K., 2002. Genogroup specific PCR primers for detection of Norwalk like viruses. J. Virol. Methods 100, 107–114.
Lamothe, G.T., Putallaz, T., Joosten, H., Marugg, J.D., 2003. Reverse transcription-PCR analysis of bottled and natural mineral waters for the presence of noroviruses. Appl. Environ. Microbiol. 69, 6541–6549.
Lew, J.F., Glass, R.I., Petric, M., LeBaron, C.W., Hammond, G.W., Miller, S.E., Robinson, C., Boutilier, J., Riepenhoff-Talty, M., Payne, C.M., Franklin, R., Oshiro, L.S., Jaqua, M.J., 1990. Six year retrospective surveillance of gastroenteritis viruses identified at ten electron microscopy centers in the United States and Canada. Pediar. Infect. Dis., 709–714.
Lewis, D.C., Lightfoot, N.F., Cubitt, W.D., Wilson, S.A., 1989. Outbreaks of astrovirus type 1 and rotavirus gastroenteritis in a geriatric in-patient population. J. Hosp. Infect. 14, 9–14.
Lindell, A.T., Grillner, L., Svensson, L., Wirgart, B.Z., 2005. Molecular epidemiology of Norovirus infections in Stockholm, Sweden, during the years 2000 to 2003: association the GGIIb genetic cluster with infection in children. J. Clin. Microbiol. 43, 1086–1092.
Logan, C., O'Leary, J.J., O'Sullivan, N., 2006a. Real-time reverse transcription-PCR for detection of norovirus, sapovirus and astrovirus as causative agents of acute viral gastroenteritis in children. J. Virol. Method. 133, 14–19.
Logan, C., O'Leary, J.J., O'Sullivan, N., 2006b. Real-time reverse transcription-PCR for detection of rotavirus and adenovirus as causative agents of acute viral gastroenteritis in children. J. Clin. Microbiol. 44, 3189–3195.
Lopman, B., Vennema, H., Kohli, E., Pothier, P., Sanchez, A., Negredo, A., Buesa, J., Schreier, E., Reacher, M., Brown, D., 2004. Increase in viral gastroenteritis outbreaks in Europe and epidemic spread of new norovirus variant. Lancet 363, 682–688.
Mackay, I.M., Arden, K.E., Nitsche, A., 2002. Real-time PCR in virology. Nucleic Acids 30, 1292–1305.
Madeley, C.R., Codgrove, B.P., 1975. 28 nm particles in feces in infantile gastroenteritis. Lancet, 451–452.
Midthun, K., Greenberg, H.B., Kurtz, J.B., Gary, G.W., Lin, F.-Y., Kapikian, Z.A., 1993. Characterization and seroepidemiology of a type 5 astrovirus associated with an outbreak of gastroenteritis in Marin Country, California. J. Clin. Microbiol. 31, 955–962.
Mitchell, D.K., Van, R., Morrow, A.L., Monroe, S.S., Glass, R.I., Pickering, L.K., 1993. Outbreaks of astrovirus gastroenteritis in day care centers. J. Pediatr. 123, 725–732.
Mitchell, D.K., Monroe, S.S., Jiang, X., Matson, D.O., Glass, R.I., Pickering, L.K., 1995. Virologic features of an astrovirus diarrhea outbreak in day care center revealed by reverse transcription-polymerase chain reaction. J. Infect. Dis. 172, 1437–1444.
Mori, K., Hayashi, Y., Sasaki, Y., Noguchi, Y., Murata, I., Morozumi, S., 2003. Community gastroenteritis caused by Adenovirus type 41. J. J. A. Inf. D. 77, 1067–1073.
Noel, J., Cubitt, D., 1994. Identification of astrovirus serotypes from children treated at the hospitals for sick children London 1981–93. Epidemiol. Infect. 113, 153–159.
Oishi, I., Yamazaki, K., Minekawa, Y., 1993. An occurrence of diarrheal cases associated with group C Rotavirus in adults. Microbiol. Immunol. 37, 505–509.
Oishi, I., Yamazaki, K., Kimoto, T., Minekawa, Y., Utagawa, E., Yamazaki, S., Inoue, S., Grohmann, G.S., Monroe, S.S., Stine, S., Carcamo, C., Ando, T., Glass, R.I., 1994. A large outbreak of acute gastroenteritis associated with astrovirus among students and teachers in Osaka, Japan. J. Infect. Dis. 170, 439–443.
Oka, T., Katayama, K., Hansman, G.S., Kageyama, T., Ogawa, S., Wu, F.T., White, P.A., Takeda, N., 2006. Detection of human sapovirus by real-time reverse transcription-polymerase chain reaction. J. Med. Virol. 78, 1347–1353.
Okada, M., Yamashita, Y., Oseto, M., Shinozaki, K., 2006. The detection of human sapoviruses with universal and genogroup-specific primers. Arch. Virol. 151, 2503–2509.
O'Neill, H.J., McCaughey, C., Coyle, P.V., Wyatt, D.E., Mitehell, F., 2002. Clinical utility of nested multiplex RT-PCR for group F adenovirus rotavirus and Norwalk-like viruses in acute viral gastroemteritis in children and adults. J. Clin. Virol. 25, 335–343.
Pang, X.I., Joensuu, J., Hoshino, Y., Kapikian, A.Z., Vesikari, T., 1999. Rotaviruses detected by reverse transcription polymerase chain reaction in acute gastroenteritis during a trial of rhesus-human reassortant rotavirus tetravalent vaccine: implications for vaccine efficacy analysis. J. Clin. Viol. 13, 9–16.
Parashar, U.D., Hummelman, E.G., Bresee, J.S., Miller, M.A., Glass, R.I., 2003. Global illness and deaths caused by rotavirus disease in children. Emerg. Infact. Dis. 9, 565–572.
Pring-Akerblom, P., Adrian, T., Kostler, T., 1997. PCR-based detection and typing of human adenoviruses in clinical samples. Res. Virol. 148, 225–231.
Putzker, M., Sauer, H., Kirchner, G., Keksel, O., Malic, A., 2000. Community acquired diarrhea-the incidence of Astrovirus infections in Germany. Clin. Lab. 46, 269–273.
Royuela, E., Negredo, A., Sanchez-Fauquier, A., 2006. Development of a one step real-time RT-PCR method for sensitive detection of human astrovirus. J. Viol. Methods 133, 14–19.
Sanchez-Fauquier, A., Roman, E., Colomina, J., Wilbelmi, I., Glass, R.I., Jiang, B., 2003. First detection of group C rotavirus in children with acute diarrhea in Spain. Arch. Virol. 148, 399–404.
Sebeta, T., Steele, A.D., 1999. Human group C rotavirus identified in South Africa. Afr. Med. J. 89, 1073–1074.
Sen, A., Kobayashi, N., Das, S., Krisman, T., Bhattacharya, S.K., Urasawa, S., Naik, T.N., 2000. Amplification of various genes of human group B rotavirus from stool specimens by RT-PCR. J. Clin. Virol. 17, 177–181.
Taylor, B.M., Marx, E.F., Grabow, K.O.W., 1997. Rotavirus, astrovirus and adenovirus associated with an outbreak of gastroenteritis in a South Africa child care centre. Epidemiol. Infect. 119, 227–230.
Texeira, J.M., Camara, G.N., Pimentel, P.F., Ferreira, M.N., Ferreira, M.S., Alfieri, A.A., Gentsch, J.R., Leite, J.P., 1998. Human group C rotavirus in children with diarrhea in the Federal District, Brazil. Braz. J. Med. Biol. Res. 31, 1397–1403.
Uhnoo, I., Wadell, G., Svenssen, L., Johansson, M.E., 1984. Importance of enteric adenoviruses 40 and 41 in acute gastroenteritis in infants and young children. J. Clin. Microbiol. 20, 365–372.
Wadell, G., 1984. Molecular epidemiology of human adenoviruses. Curr. Top Microbiol. Immunol. 110, 191–220.
Wittman, C.T., Hemann, M.G., Moss, A.A., Rasmussen, R.P., 1997. Continous fluorescence monitoring of rapid cycle DNA amplification. Biotechniques 22, 130–138.

Please cite this article in press as: Mori, K., et al., Multiplex real-time PCR assays for the detection of group C rotavirus, astrovirus, and Subgenus F adenovirus in stool specimens. J. Virol. Methods (2012), http://dx.doi.org/10.1016/j.jviromet.2012.10.019

厚生労働科学研究費補助金　肝炎等克服緊急対策研究事業
Ｂ型肝炎ウイルスｅ抗体陽性無症候性キャリアの長期予後に関する検討
平成２４年度　総括・分担研究報告書

発行日　平成25年3月
発行者　横須賀　收　（千葉大学大学院医学研究院消化器・腎臓内科学　教授）
発行所　〒260-8670 千葉県千葉市中央区亥鼻１－８－１